Ann Microbiol (2014) 64:1123–1131
DOI 10.1007/s13213-013-0751-5

ORIGINAL ARTICLE

Effect of metals ions on thermostable alkaline phytase from *Bacillus subtilis* YCJS isolated from soybean rhizosphere soil

Ming-Ze Yao · Wen-Liang Lu · Ting-Gui Chen · Wei Wang · Yue-Jun Fu · Bin-Sheng Yang · Ai-Hua Liang

Received: 22 May 2013 / Accepted: 29 October 2013 / Published online: 24 November 2013

Abstract A *Bacillus* sp.YCJS strain showing phytase activity was isolated, and the phytase-encoding gene was cloned and expressed in *Escherichia coli*. The 1,149-bp full-length gene encoded a 26-residue putative signal peptide and a 356-residue mature protein. The molecular weight was estimated to be 47.5 kDa by sodium dodecyl sulfate-polyacrylamide gel electrophoresis. The purified recombinant enzyme phy(ycE) from *E. coli* exhibited a specific activity of 14 U mg^{-1} protein. The optimum pH and temperature were 6.0 and 50 °C, respectively. The thermal stability of phy(ycE) was drastically improved in the presence of calcium ions (Ca^{2+}). Fluorescence analysis results indicated that compared with phy(ycE) without added Ca^{2+}, phy(ycE) in the presence of Ca^{2+} was more stable and the melting temperature improved from 47.8 to 62.4 °C. Circular dichroism spectrometric analysis revealed that the loss of enzymatic activity was most likely due to a conformational change, as the circular dichroism spectra of the holoenzyme and metal-depleted enzyme were significantly different. Compared with the Ca^{2+}-reactivated enzyme, the La^{3+}-reactivated enzyme did not undergo a significant recovery with respect to its conformation. The aromatic-sensitized terbium (Tb^{3+}) fluorescence results indicated that five Tb^{3+} could bind to each molecule of phy(ycE) and that there were two high-affinity and three low-affinity binding sites.

M.-Z. Yao · W.-L. Lu · W. Wang · Y.-J. Fu · A.-H. Liang (✉)
Institute of Biotechnology, Key Laboratory of Chemical Biology and Molecular Engineering of Ministry of Education, Shanxi University, 92 Wucheng Rd, Taiyuan 030006, People's Republic of China
e-mail: aliang@sxu.edu.cn

T.-G. Chen · B.-S. Yang
Institute of Molecular Science, Key Laboratory of Chemical Biology and Molecular Engineering of Ministry of Education, Shanxi University, 92 Wucheng Rd, Taiyuan 030006, People's Republic of China

Keywords Alkaline phytase · *Bacillus* · La^{3+} · Metal ions · Spectra

Introduction

Phytase catalyzes the sequential hydrolysis of phytate (myo-inositol 1,2,3,4,5,6-hexakisphosphate; IP6) to less phosphorylated myo-inositol derivatives with the concomitant release of inorganic phosphate (Oh et al. 2004). Most of the phosphorus present in plants occurs as a nonbioavailable organic complex termed phytate (Reddy et al. 1982) that also forms insoluble complexes with nutritionally important metals and proteins, thereby decreasing their bioavailability as well (Kies et al. 2006). Monogastric animals, such as humans, pigs, poultry, and fish, secrete insufficient quantities of enzymes into their digestive tracts to fully hydrolyze phytate salts and instead eliminate the mineral–phytate compounds in their feces. The loss of phytate salts contributes to the antinutritional impact of phytate and may result in mineral deficiencies in monogastric animals whose staple diet includes foods with high phytate content (Harland and Morris 1983; Bohn et al. 2008). Supplementing microbial phytases into corn–soybean meal diets for monogastric animals can reduce these problems, improve the bioavailability of minerals, and reduce their fecal phosphorus excretion by up to 50 % (Kemme et al. 1997; Liu et al. 1997). For these reasons, phytase has been used worldwide as a feed additive in the diets of swine and poultry, and even in those of aquatic animals. This has led to increased interest in the development and research of phytases (Lei and Stahl 2001).

The β-propeller phytases (BPPs) are a class of phytases that have been extensively characterized in *Bacillus* spp. In contrast to other phytases which have an acidic pH (2.5–5.5) optimum for activity, the BPPs have a neutral pH (6.0–7.5)

optimum (Oh et al. 2004). The use of *Escherichia coli* expression systems as an alternative to *Bacillus* phytase production has been extensively investigated, but the production of *Bacillus* phytase in active form in *E. coli* has met with limited success owing to the enzyme being sequestered to inclusion bodies (Kim et al. 1998; Kerovuo et al. 1998; Rao et al. 2008). The production of *Bacillus* phytase in active cell systems has been achieved (Gulati et al. 2007; Tran et al. 2010).

La^{3+} are known to exert diverse biological effects and are widely applied in the fields of agriculture and medicine for the treatment of various diseases and as a diagnostic agent in magnetic resonance imaging (Hu et al. 2004; Sudhindra et al. 2004). Due to their similarity to calcium ions (Ca^{2+}), lanthanide ions (Ln^{3+}), including those of lanthanum (La^{3+}) and terbium (Tb^{3+}), can compete with Ca^{2+} at Ca^{2+}-binding sites. Studies of several calcium-dependent proteins have revealed that Ca^{2+} can be functionally replaced by trivalent La^{3+} (Evans 1990). Here we report that the expression of Phy(ycE) in *E. coli* was about 50 % of that of the total soluble proteins. We also subjected the recombinant phytase to detailed biochemical characterization.

Materials and methods

Chemicals, plasmid, strains, and media

Phytate (dodecasodium salt from rice, P0109) was purchased from Sigma (St. Louis, MO), and all other chemicals were of analytical grade. Ultra-pure water obtained from the Millipore-MilliQ system (Millipore Corp., Billerica, MA) was used throughout the study. The pET-28a vector (TaKaRa, Kyotanabe, Japan) was used for phytase expression, and *E. coli* BL21 (DE3) (TaKaRa) cells were used as the hosts for protein expression; these cells were cultivated in/on Luria–Bertani (LB) broth/agar supplemented with ampicillin (100 μg ml^{-1}). Phytase screening medium (Howson and Davis 1983) and liquid low-phosphate medium (Makarewicz et al. 2006) were used for screening purposes. Nickel-NTA Agarose from TaKaRa was used to purify the His-tagged recombinant protein.

Production and purification of the recombinant phytase phy(ycE)

The coding sequence of the mature protein without the predicted signal peptide was inserted into the expression vector pET-28a and then introduced into *E.coli* BL21 (DE3) competent cells. The cells harboring the recombinant vector pET-phy(ycE) was cultivated in LB medium containing 100 μg ml^{-1} ampicillin (pH 7.4) at 37 °C up to an OD_{600} of 0.6–0.8. Phytase expression was induced by the addition of 0.1 mM isopropyl-β-D-1-thiogalactopyranoside (IPTG) for an additional 4 h at 37 °C. Protein expression was monitored by an activity assay and sodium dodecyl sulfate-polyacrylamide gel electrophoresis (SDS-PAGE).

To purify the recombinant His_6-tagged phytase, cells were harvested and lysed by sonication in 50 mM Tris–HCl buffer containing 5 mM $CaCl_2$ (pH 7.4). Cell debris was removed by centrifugation at 8,000 rpm for 15 min at 4 °C. The soluble fraction was loaded onto a 1-ml Nickel-NTA agarose column (Amersham Pharmacia Biotech, Uppsala, Sweden) equilibrated with binding buffer (50 mM Tris–HCl containing 5 mM $CaCl_2$, 250 mM NaCl, 5 % glycerol, pH 7.4). The column was then throughly washed with the binding buffer to remove loosely bound proteins. The protein was eluted with a linear imidazole gradient of 20–300 mM in the same buffer. Eluted fractions were analyzed by SDS-PAGE, and fractions containing pure enzyme were pooled and concentrated using the Amicon Ultra-15 Centrifugal Filter Unit equipped with an Ultracel-30 membrane (Millipore Corp.). The sample was then loaded onto a 16/60 Sephacryl S200 HR column (Amersham Pharmacia Biotech) and run on the AKTA FPLC system (GE, Amersham, Little Chalfont, UK). The protein concentration of the purified enzyme was determined by the Bradford assay, using bovine serum albumin as a standard (Asryants et al. 1985).

Phytase activity assay

Phytase activity of the recombinant phy(ycE) was assayed by measuring the rate of increase in inorganic orthophosphate (Pi) level using the ferrous sulfate–molybdenum blue method (Holman 1943; Zhang et al. 2011). One unit (U) of phytase activity was defined as the amount of enzyme that released 1 μmol phosphate per minute at 37 °C. All phytase activity determinations were performed in triplicate.

Biochemical characterization of purified recombinant phy(ycE)

The properties of purified recombinant phytases were determined using 1.5 mM phytate as the substrate. The optimal concentration of Ca^{2+} for phytase activity of phy(ycE) was determined at 37 °C in 100 mM Tris–HCl (pH 7.4) containing different concentrations (0–5.0 mM) of Ca^{2+}.

The thermal stability was estimated by measuring the residual enzyme activity after pre-incubating the enzyme in 100 mM Tris–HCl (pH 7.4) supplemented with various concentrations of Ca^{2+} (0, 1, 5, and 10 mM) at 75 °C for various lengths of time. Residual enzyme activity was then assayed under standard conditions (pH 7.4, 37 °C, 15 min). To determine the effects of metal ions and chemicals on phy(ycE) activity, phytase activity was also assayed in the presence of each reagent of interest (at 1 or 5 mM concentration).

The kinetic values of K_m (Michaelis constant), V_{max} (maximum rate), and k_{cat} (catalytic constant) for the purified recombinant phytases were measured by the Lineweaver–Burk method (Lineweaver and Burk 1934). The phytase activity was determined in 100 mM Tris–HCl (pH 7.4) containing various concentrations of phytate (0.25–3 mM) with the same concentration of Ca^{2+} at 37 °C for 5 min.

Metal depletion and reactivation of apoenzyme

Metal-depleted enzyme (apoenzyme) was prepared by incubating native enzyme (holoenzyme) in 10 mM EDTA, 100 mM Tris–HCl, pH 7.4, at 4 °C for 5 h, concentrating it using the Amicon Ultra-15 centrifugal filter unit equipped with the Ultracel-30 membrane (Millipore Corp.), and loading it onto a Hiprep 26/10 desalting column (Pharmacia, Stockholm, Swede) pre-equilibrated with EDTA free Tris–HCl buffer, pH 7.4.

Activation by Ca^{2+}

The apo-phytase was pre-incubated with increasing amounts of Ca^{2+} followed by the addition of phytate pre-incubated with the same concentration of Ca^{2+}. The experiments were conducted in 100 mM Tris–HCl (pH 7.4) containing 0–1.5 mM Ca^{2+} at 37 °C. The interaction between Ca^{2+} and the apo-phytase was monitored in 100 mM Tris–HCl at pH 7.4 by native PAGE. The protein concentration was 4.8×10^{-6} M.

The activation of metal ions on phytase activity

Apoenzyme was reactivated by incubating it with various cations (Ca^{2+}, Sr^{2+}, Co^{2+}, Ba^{2+}, Cu^{2+}, La^{3+}, Ni^{+}, Tb^{2+}, Li^{+}, Mg^{2+}, Na^{+}, Mn^{2+}, Fe^{2+}, Zn^{2+}, Fe^{3+} as chlorides) at a concentration of 2 mM at 4 °C overnight. The protein concentration was 4.8×10^{-6} M.

Circular dichroism spectroscopy

The circular dichroism (CD) spectra of the holoenzyme, apoenzyme, calcium-reactivated enzyme, and lanthanum-reactivated enzyme were obtained on a MOS-450 spectrometer (Bio-Logic Science Instruments Corp., Claix, France). Spectra were obtained at 25 °C using a 1-cm path-length quartz cuvette. Each spectrum represents the average of three accumulations recorded between 195 and 250 nm, with readings taken at 1-nm intervals, and a scan speed of 50 nm min^{-1}. All spectra were run in the same buffer (10 mM Tris–HCl, pH 7.4) and at a protein concentration of 2×10^{-6} M.

Fluorescence measurements

Fluorescence spectra were measured using a Cary Eclipse Fluorescence spectrophotometer equipped with a temperature controller (Varian Medical Systems, Palo Alto, CA). Protein samples (2.8×10^{-5} M) were prepared in 100 mM Tris–HCl buffer (pH 7.4) containing 0, 1, 5, or 10 mM $CaCl_2$. The emission spectra (300–540 nm) were performed by raising the temperature from 10 to 95 °C at a rate of 5 °C per 3 min using an excitation wavelength of 280 nm. The slit widths for excitation and emission were 5 nm. The melting temperature (T_m) values of the melting curves with different Ca^{2+} were calculated by performing Curve-fitting using SigmaPlot (Systat Software, San Jose, CA) .

Binding of Tb^{3+} to phy(ycE)

The aromatic residue-sensitized Tb^{3+} fluorescence spectra were measured from 475–565 nm with excitation at 295 nm using a Hitachi F-2500 fluorescence spectrophotometer (Hitachi, Tokyo, Japan). The slit widths for excitation and emission were 5 nm. Protein samples (2.8×10^{-5} M) were prepared in 100 mM Tris–HCl buffer (pH 7.4).

Docking La^{3+} into myo-inositol hexasulfate-phytase

Surflex-Dock computational high-throughput screening (Tripos Int., St. Louis, MO) integrated in SYBYL-X 1.2 software was used to explore the binding of myo-inositol hexasulfate (IHS) to Ca^{2+}-loaded and La^{3+}-loaded phytase, respectively. The Surflex-Dock system has been extensively validated and favorably compares to all leading competing methods (Kellenberger et al. 2004). As a first step towards homology modeling, the template structure was identified from the Protein Data Bank (PDB) using NCBI-BLAST (http://www.ncbi.nlm.nih.gov/BLAST/). The phytase structure with the highest sequence identity and resolution was selected as a template structure for modeling (PDB ID: 3AMR). Sequence analysis and homology modeling were performed using the software Insight II 2005 (Accelrys, San Diego, CA). The phytase model was manually inspected for accuracy and validity using SYBYL-X 1.2 software which calculates a three-dimension to one-dimension compatibility score. The graphical representation in the output shows both correctly folded and misfolded regions in the protein structure based on an Eisenberg analysis of the model. The stereochemistry of the model was further gauged using a Ramachandran plot on the PROCHECK function implemented in the SYBYL-X 1.2 program. Surflex-Dock from the SYBYL-X 1.2 program was used to dock La^{3+} into the IHS-phytase and to investigate H-bond formation in the calcium-phytase and lanthanum-phytase.

Results

Production and purification of recombinant phy(ycE)

The recombinant plasmid pET-phy(ycE) was constructed and transformed into *E. coli* BL21 (DE3). Positive transformants harboring the recombinant plasmid pET-phy(ycE) were induced with 0.1 mM IPTG at 37 °C for 4 h. *Bacillus* sp. YCJS phytase, expressed in a soluble and active form in *E. coli* BL21 (DE3) cells, was purified to homogeneity using a two-step procedure involving immobilized metal ion affinity chromatography and size exclusion chromatography (Fig. 1). The pure recombinant enzyme had a specific activity of 14 U mg^{-1} and a molecular weight of about 47.5 kDa.

Biochemical characterization of purified recombinant phy(ycE)

Ca^{2+} plays an important role in the catalytic activity and thermostability of BPPs (Oh et al. 2001). Therefore, we assayed the phytase activity of the purified phy(ycE) in the presence of Ca^{2+} concentrations ranging from 0 to 5 mM. Very little activity was detected when the phytase was added to phytate in the Ca^{2+}-free environment, and a drastic increase in activity was observed at 1.5 mM Ca^{2+} (Fig. 2a). Based on these results, we characterized other properties of purified phy(ycE) in the presence of 1.5 mM Ca^{2+}.

Purified phy(ycE) showed optimal activity at pH 6.0 and at this pH the optimum temperature was 50 °C. A pH stability test indicated that the phytase activity of Phy(ycE) was stable under alkaline conditions(data not shown). The phy(ycE) showed variable thermal stability at different Ca^{2+} concentrations, with the thermal stability of the enzyme increasing at higher Ca^{2+} concentrations (Fig. 2b). The enzyme lost >75 % of its activity after incubation at 75 °C for 5 min in the absence of Ca^{2+}, whereas >60 % of the activity was retained in the presence of 10 mM Ca^{2+} at 75 °C for 10 min. The phytase activity of the phy(ycE) in the presence of 1 or 5 mM of different metal ions or chemical reagents was also assayed. There was little enhancement of phytase activity in the presence of K^+, Li^+, Mg^{2+}, Fe^{3+}, and Ba^{2+}, a strong inhibition of activity in the presence of Cu^{2+} and Ag^+, and a complete inhibition of activity in the presence of Cr^{3+} and Pb^{2+}. Phytase activity was also decreased by a number of other chemicals tested (1 mM or 5 mM each). In contrast, the activity of fungal and *E. coli* phytases is known to be completely inhibited by SDS and enhanced slightly by EDTA (Haefner et al. 2005). The addition of the other metal ions tested had little effect on phytase activity. The kinetic parameters of the enzyme with respect to sodium phytate were calculated from a Lineweaver–Burk plot. The K_m, V_{max}, and k_{cat} values were 0.36 mM, 1.05 umol min^{-1} mg^{-1}, and 25.4 s^{-1}, respectively. The specific activity of the phy(ycE) was 14 U mg^{-1} at the optimal Ca^{2+} concentration.

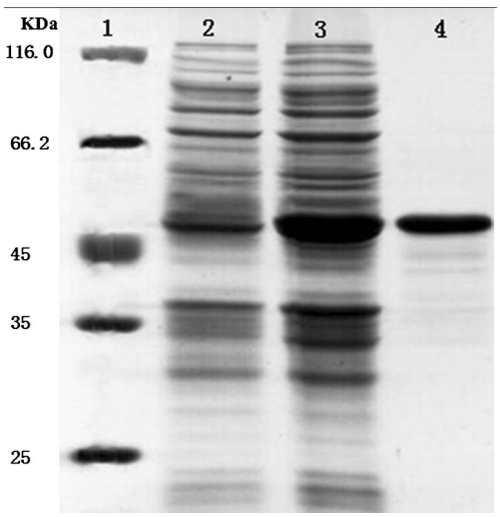

Fig. 1 Sodium dodecyl sulfate-polyacrylamide gel electrophoresis (SDS-PAGE) analysis of the expression and purification of the recombinant phytase [phy(ycE)] from *Escherichia coli* BL21 (DE3). *Lanes*: *1* Prestained molecular weight markers, *2* culture supernatant of induced transformant harboring the empty plasmid, *3* culture supernatant of the induced transformant harboring the recombinant plasmid pET-phy(ycE), *4* purified recombinant phy(ycE) obtained using a two-step procedure

Metal depletion and reactivation of apoenzyme

When the apo-phytase was incubated with varying concentrations of Ca^{2+} (range0–1.5 mM) overnight at 4 °C, the enzyme activity were measured by the addition of phytate pre-incubated with the same concentration of Ca^{2+}. No phytase activity was detected for the apo-Phy(ycE) in the absence of Ca^{2+}, and increases in the concentration of Ca^{2+} enhanced phytase activity, with a final plateau reached at 1 mM Ca^{2+} (Fig. 3a). Increases in the concentration of Ca^{2+} resulted in the appearance of a new protein band in some lanes whose mobility was slightly slower than that of phy(ycE), indicating the formation of a new complex. The intensity of this new band also nearly reached maximal intensity at Ca^{2+} concentration of 1 mM. No other complexes of different stoichiometries were observed (Fig. 3b). The metal-depleted apoenzyme was incubated with various divalent metal ions in order to reactivate the enzyme (Table 1). We found that no re-activation was obtained with Li^+, Mg^{2+}, Na^+, Fe^{2+}, and Zn^{2+} and Fe^{3+}, while Ca^{2+}, Sr^{2+},Co^{2+}, Ba^{2+}, Cu^{2+}, La^{3+}, Ni^+, Tb^{2+}, and Mn^{2+} restored enzyme activity to 44.1, 29.8, 36.7, 26.9,1.9 %, 30.0, 34.2, 8.3, and 34.9 % of its reference activity. No reactivation was obtained in the absence of divalent metal ions.

CD spectroscopy

Circular dichroism was used to characterize the distribution of the secondary structural elements in Phy(ycE) and to determine whether any changes occurred upon binding the metal

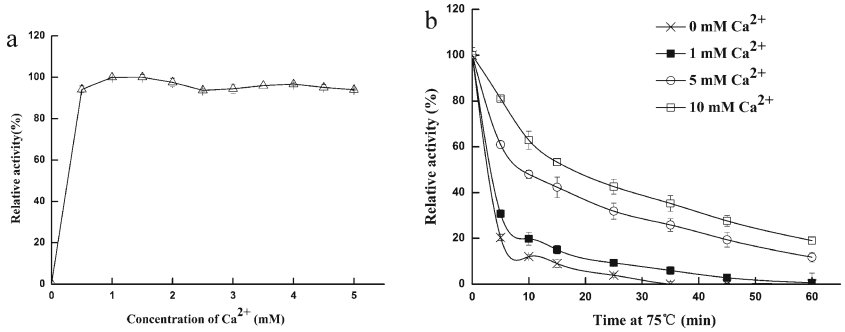

Fig. 2 Characterization of the purified recombinant phy(ycE). **a** Effect of calcium ion (Ca^{2+}) concentration on phytase activity. The assay was performed at 37 °C and at different Ca^{2+} concentrations ranging from 0 to 5 mM. **b** Thermal stability of phy(ycE). The enzyme was incubated at 75 °C in 100 mM Tris–HCl (pH 7.4) containing 0–10 mM Ca^{2+} for various lengths of time, and the residual activity was determined at 37 °C and pH 7.4 for 15 min. Each value in the panels represents the mean ± SD (n = 3)

ion with protein. CD-spectra of the holoenzyme, apoenzyme, Ca^{2+}-reactivated enzyme, and La^{3+}-reactivated enzyme were run (Fig. 4). The CD study shows that the removal of Ca^{2+} caused a change in the CD-spectrum. This kind of intensity difference in the CD-spectrum of the Ca^{2+}-bound and apoenzyme has been reported for *Bacillus subtilis* phytase (Kerovuo et al. 2000). There is a clear difference in the 205- to 220-nm region between the holoenzyme and apoenzyme. The addition of Ca^{2+} to the apoenzyme resulted in an increase in the mean residue ellipticity, indicating a recovery of β-sheet elements. In striking contrast, no such effect was observed for the lanthanum-reactivated enzyme.

Fluorescence measurements

Fluorescence spectra have been used to evaluate the thermal unfolding and refolding of phytase (Wyss et al. 1998; Shim and Oh 2012). To investigate the structural properties and conformational changes of phy(ycE) at various Ca^{2+} concentrations (0, 1, 5, and 10 mM), the thermal denaturation of phy(ycE) by heating was analyzed by tryptophan fluorescence (Fig. 5). The results fo the fluorescence analyses indicate that when the enzyme was incubated in 100 mM Tris–HCl (pH 7.4) supplemented with various Ca^{2+} concentrations and then subjected to increases in temperature from 10 to 95 °C at a scan rate of 5 °C/3 min, the fluorescence emission intensity gradually decreased with increasing temperature. The apparent effect of calcium ions on Phy(ycE) thermal stability was measured in the presence of various Ca^{2+} concentrations, while a drastic transition in fluorescence emission intensity was observed in the temperature range from 50 to 70 °C. The T_m values for Ca^{2+} concentrations of 0, 1, 5, and 10 mM were 47.8, 52.8, 57.2, and 62.4 °C, respectively.

Tb^{3+} has been widely used to identify Ca^{2+}-binding proteins (Wang et al. 2007, 2008; Hogue et al. 1992). When Tb^{3+} is added to the protein solution, the sensitized emission of Tb^{3+} at 545 nm is measured as the protein is irradiated at 280 nm in the tyrosine/tryptophan absorption band. The titration curves of Tb^{3+}-sensitized emission at 545 nm versus [Tb^{3+}]/[protein] were produced for phy(ycE). As shown in Fig. 6, fluorescence sensitivities were induced substantially with the addition of the first two equivalents of Tb^{3+}. With the addition of another three equivalents of Tb^{3+}, binding appeared to be quantitatively, but with minimal sensitization, and a final plateau was reached at the [Tb^{3+}]/[protein] ratio of five. The titration curves revealed two breaks at r = ~2 and r =

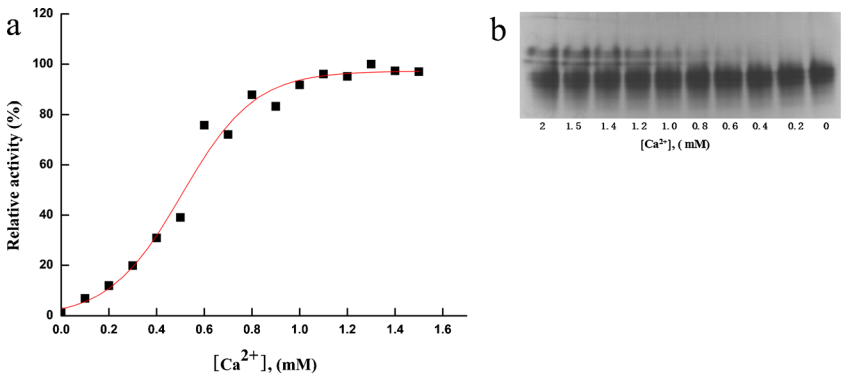

Fig. 3 Reactivation of phytase activity in the presence of Ca^{2+}. **a** The apo-phy(ycE) was pre-incubated with increasing concentrations of Ca^{2+} followed by the addition of 1.5 mM phytate pre-incubated with the same concentration of Ca^{2+} at 100 mM Tris–HCl (pH 7.4). **b** Native PAGE of Ca^{2+} binding with apo-phy(ycE). The enzyme (4.8 nM) was incubated at 4 °C in 100 mM Tris–HCl buffer (pH 7.4) supplemented with different Ca^{2+} concentrations (0, 0.2, 0.4, 0.6, 0.8, 1.0, 1.2, 1.4, 1.5, and 2.0 mM)

Table 1 Effects of metal ions on the phytase activity of the metal-depleted recombinant phytase phy(ycE)

Metal ion	Relative activity (%)[a] 2 mM	Metal ion	Relative activity (%) 2 mM
Control	100.0 ± 1.8	Tb^{2+}	8.3±0.5
Ca^{2+}	44.1±2.4	Li^{+}	0.0±0
Sr^{2+}	29.8±0.5	Mg^{2+}	0.0±0
Co^{2+}	36.7±1.1	Na^{+}	0.0±0
Ba^{2+}	26.9±2.5	Mn^{2+}	34.9±0.6
Cu^{2+}	1.9±0.3	Fe^{2+}	0.0±0
La^{3+}	30.0±2.0	Zn^{2+}	0.0±0
Ni^{+}	34.2±1.0	Fe^{3+}	0.0±0

[a] Relative activity (percentage) is given as the mean of triplicates

~5, confirming the 5:1 stoichiometric ratio of the Tb_5–phy(ycE) complex and the presence of two high-affinity and three low-affinity sites.

Docking La^{3+} into IHS-phytase

Validation of the phy(ycE) homology model showed reliable folding and stereochemistry of the constructed protein structure (data not show). The conformation with the best binding score was checked against the IHS-phytase co-crystallized with divalent metal ions (PDB ID: 3AMR) (Zeng et al. 2011). Molecular modeling of the docking Ca^{2+} into IHS-phytase shows that IHS was able to form four hydrogen bonds with the K49, K152, R95. However, docking La^{3+} into IHS-phytase shows that IHS was able to form seven hydrogen bonds with the K49, K152, R95 when compared with that of Ca^{2+} (Fig. 7a,b).

Discussion

We report her our cloning of a BPP gene (JQ 257502) from *B. subtilis* YCJS, a strain isolated from soybean rhizosphere soil. *Bacillus* species constitute an important source of alkaline phytases, which are highly homologous to each other. The deduced amino acid sequence of phy(ycE) has it highest identity (98 %) with pSPHY(Rao et al. 2008). However, *pSPHY* was expressed in *E.coli* in the insoluble cytoplasmic fraction as inclusion bodies. In striking contrast, when the transformed *E. coli* expressing phy(ycE) was cultured in the shake-flask cultures, the amount of the soluble fusion protein was about 50 % of the amount of large intestine *Bacillus* soluble protein of the transformed cells, as estimated by absorbance scanning of SDS-PAGE bands and protein quantitation. *Bacillus* phytase has been shown to be very sensitive to commonly used chromatographic purification methods, such as ion exchange and gel filtration (Kerovuo et al. 1998). Therefore, dissolving $CaCl_2$ in all of the purification steps in order to maintain activity proved to be the best purification method and for this reason was used to purify protein for enzyme characterization. Phy(ycE), like the majority of *Bacillus* phytases, was optimally active at a neutral pH (pH 6.0–7.5) (Kerovuo et al. 1998; Farhat et al. 2008). Despite phy(ycE) differing from the mature protein region within the *pSPHY* gene encoding the phytase pSPHY of *B. subtilis* by only six amino acids (Rao et al. 2008), these two proteins differ in a number of enzymology properties. The phy(ycE) protein displayed optimum activity at pH 6.0 versus the optimum pH of 7.0 for pSPHY. In addition, phy(ycE) exhibited activity in a broad pH range (5.0–9.5), which is of crucial importance as the pH of the animal gastrointestinal tract ranges from 2.6 to 7.0 (range 4.0–5.0 in the stomach in the presence of food).

The enzymatic activity could be restored only partially by the addition of Ca^{2+} following the deletion of Ca^{2+} (Table 1). Increasing the concentration of Ca^{2+} enhanced phytase activity in a saturating manner (Fig. 3a). These data are consistent with the results of native PAGE, suggesting that calcium specifically induces a conformational change in phy(ycE) (Fig. 3b). Replacing calcium on the phy(ycE) enzyme with other cations resulted in either partial activation and no activation at all. These results are similar with earlier reports of a partial recovery of *B. subtilis* PhyC activity upon reactivation by Ca^{2+} and only limited recovery by Ni^{2+}, Mn^{2+}, and Co^{2+}. Oh et al. (2001) reported the partial activation of *Bacillus* DS11 phytase with Sr^{2+} but not with any other cation. Our observations differ from earlier studies that showed partial activation of TS-Phy phytase with Mg^{2+} and no activation with other metal ions (Co^{2+}, Ni^{+}, and Mn^{2+}) (Ha et al. 2000; Oh et al. 2001). We compared and contrasted the effects of Ca^{2+} and La^{3+}on the protein conformation, CD-spectra of the holoenzyme, apoenzyme, Ca^{2+}-reactivated enzyme, and La^{3+}-reactivated enzyme. As shown in Fig. 4, CD signals of phy(ycE) decreased significantly with demetalization of Ca^{2+}. We also found that the conformation of the Ca^{2+}-reactivated enzyme, unlike that of the La^{3+}-reactivated

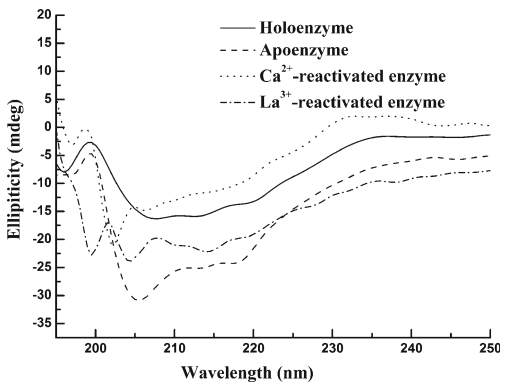

Fig. 4 Far-UV circular dichroism spectra of the 2.0 nM phytase in 10 mM Tris–HCl buffer (pH 7.4)

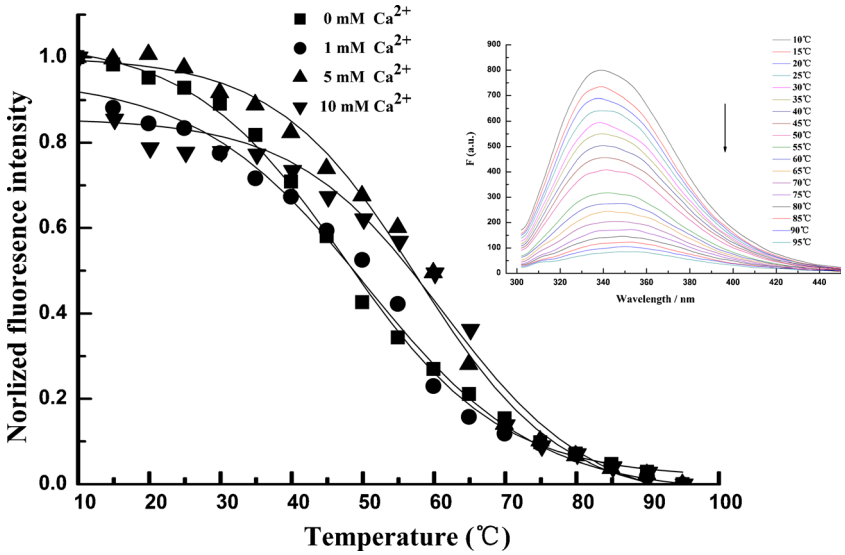

Fig. 5 The effect of changes in temperature on the fluorescence emission of phy(ycE). Emission spectra (300–540 nm) were analyzed at temperatures ranging from 10 to 95 °C, with a heating rate of 5 °C/3 min and at an excitation wavelength of 280 nm. Fluorescence spectra were measured in the presence of varying concentrations of Ca^{2+}. The melting temperature (T_m) values of the melting curves with different Ca^{2+} were calculated by performing Curve-fitting using SigmaPlot

enzyme, underwent a significant recovery, suggesting that the conformational change induced by calcium is specific to phy(ycE), although La^{3+} restored enzyme activity to 30.0 %. The mechanism by which La^{3+} modulates enzyme activity might differ from that of Ca^{2+}. Figure 6 shows that there are five-binding sites for Tb^{3+} in phy(ycE) and that the binding sites can be divided into two classes. At a stoichiometry of two Tb^{3+} per molecule of phy(ycE), there is a great change in fluorescence, suggesting that Tb^{3+} bound first to the strong binding sites a with strong sensitization for Tb^{3+} fluorescence. The addition of another three ions of Tb^{3+} per molecule of phy(ycE) produced only a slight increase in fluorescence: three weak binding sites with a weak sensitization for Tb^{3+} fluorescence. As is well known, Tb^{3+}, due to its similarity to Ca^{2+} in coordination chemistry, can compete with Ca^{2+} at calcium-binding sites. Thus, Tb^{3+} is assumed to bind to the same Ca^{2+} loci. This observation coincides with early results that BPPs possess two classes of Ca^{2+}-binding sites (Ha et al. 2000; Shin et al. 2001; Zeng et al. 2011). However, no difference was detected in the activities of phy(ycE) in the presence of Tb^{3+} and phy(ycE) in the absence of Tb^{3+}($p > 0.05$). Therefore, Tb^{3+} may play an integral role outside the active site, which may be classified into the high-affinity sites and low-affinity sites.

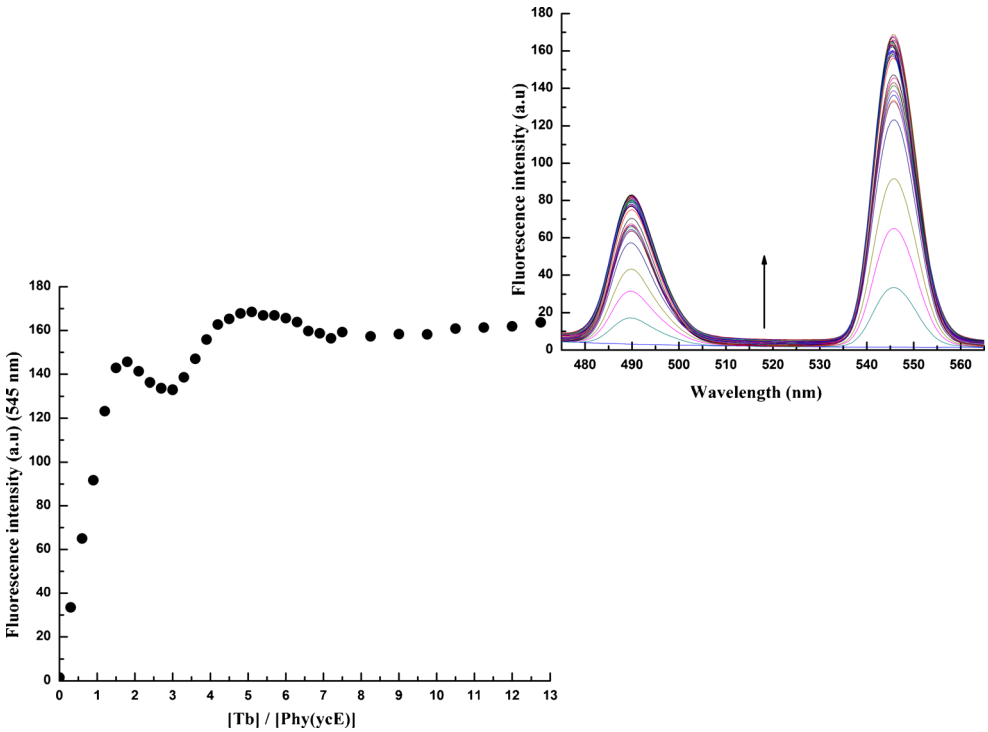

Fig. 6 Titration curves of the of Tb^{3+}-sensitized fluorescence emission at 545 nm following the addition of terbium ions (Tb^{3+}) to phy(ycE). The concentration of phy(ycE) was 28 nM in 100 mM Tris–HCl buffer (pH 7.4)

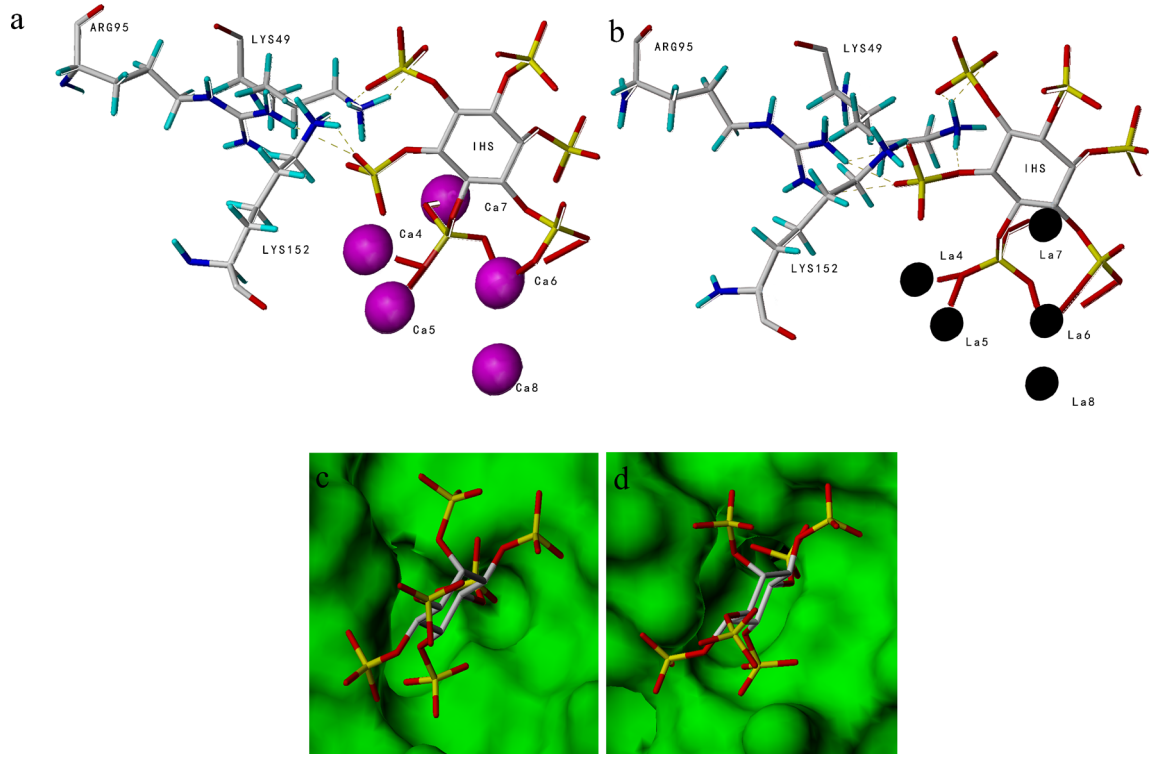

Fig. 7 Probing the binding of myo-inositol hexasulfate (IHS) to Ca^{2+}- and La^{3+}-phytase. **a**, **b** Top view of IHS docked into Ca^{2+}-loaded phytase and La^{3+}-loaded phytase. *Dashed lines* Hydrogen bonds. **c**,**d** Surface representation of the binding of IHS to Ca^{2+}- and La^{3+}-phytase

Investigating the effect of La^{3+} on phytase would be of interest since with their very similar ion radii (1.03 Å) and similar coordination numbers, the La^{3+} can replace Ca^{2+} in proteins even though they exhibit different charges. The effect of La^{3+} on the binding of IHS was explored using SYBYL-X 1.2 software and compared with that of Ca^{2+}. The software successfully predicted the binding of IHS to the cleavage site and binding site in the presence of Ca^{2+}, which is in line with the findings of Zeng et al. (2011). However, docking La^{3+} into IHS-phy(ycE) increases the number of hydrogen bonds which may in turn over-stabilize the phytate–enzyme intermediate and result in decreased enzyme activity. The findings of Tomschy et al. (2000) confirmed this hypothesis, as these authors observed an increase in the specific activity of *Aspergillus fumigatus* phytase with the Q27L mutation, which was interpreted as a direct effect of the removal of hydrogen bonding between glutamine and phytate . Moreover, the restored activity of Ca^{2+}-phytase was higher than that of La^{3+}-phytase, which was also confirmed by a better fitting of the IHS to the active site of the Ca^{2+}-phytase in comparison to the La^{3+}-phytase. The HIS of the La^{3+}-phytase has a deeper cover and is located in the catalytic pocket when compared with that of Ca^{2+} (Fig. 7c, d). A recent study has shown similar results for Zn^{+2}-loaded phytase: phosphate group is not properly placed in the cleavage site of the phytase. The disoriented position of IP6 does not allow the stabilization of the pentavalent transitional state, which could explain the loss of activity in the case of Zn^{2+}(Tran et al. 2011). Based on our study of La^{3+}, further studies should focus on mutagenic and structural analyses of the enzyme with the aim of gaining a full understanding of the interactions with Tb^{2+}, La^{3+} and the effects thereof.

Acknowledgments This work was supported by grants from the "National Natural Science Foundation of China" (No. 31071924, 31272100), the "Natural Science Foundation of Shanxi Province" (2010011040–1), and the "Shanxi Scholarship Council of China". We are grateful to Prof. Daxiong Han from Medical College Xiamen University for software support.

References

Asryants RA, Duszenkova IV, Nagradova NK (1985) Determination of Sepharose-bound protein with Coomassie brilliant blue G-250. Anal Biochem 151(2):571–574

Bohn L, Meyer AS, Rasmussen SK (2008) Phytate: impact on environment and human nutrition. A challenge for molecular breeding. J Zhejiang Univ Sci B 9(3):165–191

Evans CH (1990) Biochemistry of the lanthanides. Plenum Press, New York

Farhat A, Chouayekh H, Ben Farhat M, Bouchaala K, Bejar S (2008) Gene cloning and characterization of a thermostable phytase from *Bacillus subtilis* US417 and assessment of its potential as a feed

additive in comparison with a commercial enzyme. Mol Biotechnol 40(2):127–135

Gulati HK, Chadha BS, Saini HS (2007) Production and characterization of thermostable alkaline phytase from *Bacillus laevolacticus* isolated from rhizosphere soil. J Ind Microbiol Biotechnol 34(1):91–98

Ha NC, Oh BC, Shin S, Kim HJ, Oh TK, Kim YO, Choi KY, Oh BH (2000) Crystal structures of a novel, thermostable phytase in partially and fully calcium-loaded states. Nat Struct Biol 7(2):147–153

Haefner S, Knietsch A, Scholten E, Braun J, Lohscheidt M, Zelder O (2005) Biotechnological production and applications of phytases. Appl Microbiol Biotechnol 68(5):588–597

Harland BF, Morris ER (1983) Phytate: a good or a bad food component. Nutr Res Rev 15:733–754

Hogue CW, MacManus JP, Banville D, Szabo AG (1992) Comparison of terbium (III) luminescence enhancement in mutants of EF hand calcium binding proteins. J Biol Chem 267(19):13340–13347

Holman WI (1943) A new technique for the determination of phosphorus by the molybdenum blue method. Biochem J 37(2):256–259

Howson SJ, Davis RP (1983) Production of phytate-hydrolysing enzyme by some fungi enzyme. Microbiol Technol 5:377–382

Hu J, Jia X, Li Q, Yang X, Wang K (2004) Binding of La^{3+} to calmodulin and its effects on the interaction between calmodulin and calmodulin binding peptide, polistes mastoparan. Biochemistry 43(10):2688–2698

Kellenberger E, Rodrigo J, Muller P, Rognan D (2004) Comparative evaluation of eight docking tools for docking and virtual screening accuracy. Proteins 57(2):225–242

Kemme PA, Radcliffe JS, Jongbloed AW, Mroz Z (1997) The effects of sow parity on digestibility of proximate components and minerals during lactation as influenced by diet and microbial phytase supplementation. J Anim Sci 75(8):2147–2153

Kerovuo J, Lauraeus M, Nurminen P, Kalkkinen N, Apajalahti J (1998) Isolation, characterization, molecular gene cloning, and sequencing of a novel phytase from *Bacillus subtilis*. Appl Environ Microbiol 64(6):2079–2085

Kerovuo J, Lappalainen I, Reinikainen T (2000) The metal dependence of *Bacillus subtilis* phytase. Biochem Biophys Res Commun 268(2): 365–369

Kies AK, De Jonge LH, Kemme PA, Jongbloed AW (2006) Interaction between protein, phytate, and microbial phytase. In vitro studies. J Agric Food Chem 54(5):1753–1758

Kim YO, Lee JK, Kim HK, Yu JH, Oh TK (1998) Cloning of the thermostable phytase gene (phy) from *Bacillus* sp. DS11 and its overexpression in *Escherichia coli*. FEMS Microbiol Lett 162(1): 185–191

Lei XG, Stahl CH (2001) Biotechnological development of effective phytases for mineral nutrition and environmental protection. Appl Microbiol Biotechnol 57(4):474–481

Lineweaver H, Burk D (1934) The determination of enzyme dissociation constants. J Am Chem Soc 56:658–666

Liu J, Bollinger DW, Ledoux DR, Ellersieck MR, Veum TL (1997) Soaking increases the efficacy of supplemental microbial phytase in a low-phosphorus corn-soybean meal diet for growing pigs. J Anim Sci 75(5):1292–1298

Makarewicz O, Dubrac S, Msadek T, Borriss R (2006) Dual role of the PhoP approximately P response regulator: *Bacillus amyloliquefaciens* FZB45 phytase gene transcription is directed by positive and negative interactions with the phyC promoter. J Bacteriol 188(19):6953–6965

Oh BC, Chang BS, Park KH, Ha NC, Kim HK, Oh BH, Oh TK (2001) Calcium-dependent catalytic activity of a novel phytase from *Bacillus amyloliquefaciens* DS11. Biochemistry 40(32):9669–9676

Oh BC, Choi WC, Park S, Kim YO, Oh TK (2004) Biochemical properties and substrate specificities of alkaline and histidine acid phytases. Appl Microbiol Biotechnol 63(4):362–372

Rao DE, Rao KV, Reddy VD (2008) Cloning and expression of *Bacillus* phytase gene (phy) in *Escherichia coli* and recovery of active enzyme from the inclusion bodies. J Appl Microbiol 105(4):1128–1137

Reddy NR, Sathe SK, Salunkhe DK (1982) Phytates in legumes and cereals. Adv Food Res 28:1–92

Shim JH, Oh BC (2012) Characterization and application of calcium-dependent beta-propeller phytase from *Bacillus amyloliquefaciens* DS11. J Agric Food Chem 60:7532–7537

Shin S, Ha NC, Oh BC, Oh TK, Oh BH (2001) Enzyme mechanism and catalytic property of beta propeller phytase. Structure 9(9):851–858

Sudhindra NM, Minaz AG, Indira DM, Ram SS (2004) Biological and clinical aspects of lanthanide coordination compounds. Bioinorg Chem Appl 2(3–4):155–192

Tomschy A, Tessier M, Wyss M, Brugger R, Broger C, Schnoebelen L, van Loon AP, Pasamontes L (2000) Optimization of the catalytic properties of *Aspergillus fumigatus* phytase based on the three-dimensional structure. Protein Sci Publ Protein Soc 9(7):1304–1311

Tran TT, Mamo G, Mattiasson B, Hatti-Kaul R (2010) A thermostable phytase from *Bacillus* sp. MD2: cloning, expression and high-level production in *Escherichia coli*. J Ind Microbiol Biotechnol 37(3): 279–287

Tran TT, Hashim SO, Gaber Y, Mamo G, Mattiasson B, Hatti-Kaul R (2011) Thermostable alkaline phytase from *Bacillus* sp. MD2: effect of divalent metals on activity and stability. J Inorg Biochem 105(7): 1000–1007

Wang ZJ, Ren LX, Zhao YQ, Li GT, Liang AH, Yang BS (2007) Metal ions-induced conformational change of P23 by using TNS as fluorescence probe. Spectrochim Acta A Mol Biomol Spectrosc 66(4–5):1323–1326

Wang ZJ, Ren LX, Zhao YQ, Li GT, Duan L, Liang AH, Yang BS (2008) Investigation on the binding of TNS to centrin, an EF-hand protein. Spectrochim Acta A Mol Biomol Spectrosc 70(4):892–897

Wyss M, Pasamontes L, Remy R, Kohler J, Kusznir E, Gadient M, Muller F, van Loon A (1998) Comparison of the thermostability properties of three acid phosphatases from molds: *Aspergillus fumigatus* phytase, *A. niger* phytase, and *A. niger* PH 2.5 acid phosphatase. Appl Environ Microbiol 64(11):4446–4451

Zeng YF, Ko TP, Lai HL, Cheng YS, Wu TH, Ma Y, Chen CC, Yang CS, Cheng KJ, Huang CH, Guo RT, Liu JR (2011) Crystal structures of *Bacillus* alkaline phytase in complex with divalent metal ions and inositol hexasulfate. J Mol Biol 409(2):214–224

Zhang R, Yang P, Huang H, Yuan T, Shi P, Meng K, Yao B (2011) Molecular and biochemical characterization of a new alkaline beta-propeller phytase from the insect symbiotic bacterium *Janthinobacterium* sp. TN115. Appl Microbiol Biotechnol 92(2): 317–325